

# STATUS OF OPERATIONAL AMVs FROM FY-2C

Xu Jianmin   Zhang Qisong   Zhang Xiaohu   Wang Sujuan   Lu Feng

National Satellite Meteorological Center  
China Meteorological Administration

## ABSTRACT

FY-2C is the first operational meteorological satellite of China. FY-2C was launched on 19 Oct 2004. From 1 Jan 2005 on, FY-2C broadcasts data. From 1 June 2005 on, FY-2C distributes products. AMV is one of the FY-2C products. From 25 Nov 2005 on, BUFR code of FY-2C AMVs is transmitted through GTS. This paper briefly introduces NSMC AMV derivation algorithm and performance.

Image navigation and calibration performance influences AMV quality greatly. Automatic image navigation accuracy for FY-2C images reaches pixel level. Inter calibrations between FY-2C and NOAA observations are performed. Infrared and water vapour channel calibrations are compatible with NOAA observations.

The major components of the NSMC processing include tracer selection, tracer tracking, height assignment and horizontal consistence examination.

In height assignment component, distinction between high and low clouds is made before height adjustment by correlation between the IR and WV matching templates; opaque cloud radiation is calculated with NWP data by using radiation model.

Time consistency examination is performed immediately after tracer tracking; horizontal consistency examination and height adjustment are performed immediately after height assignment. Tracers failed in the examinations are eliminated.

Quality and reliability of FY-2C AMVs are estimated by comparison with winds from radiosonde observations. Monthly statistics is shown.

### 1. FY-2C Navigation and Calibration Status

High quality image navigation and calibration are bases for AMV derivation.

Image navigation is a major part of the FY-2 observation process and is based on a mathematical model. The model uses time series of satellite positions and observation vectors toward earth center as input. Image grids in the future 24 hours are predicted automatically. Image navigation accuracy depends on ranging and observation quality. In case 3 hourly ranging and hourly full disk images of the previous day are well performed, and except for 48 hours after orbital and attitude control, FY-2 image navigation accuracy approaches 1 IR pixel or 2 visible pixels. During eclipse periods, two midnight images are not taken, the accuracy is around 1 IR pixel. In successive images navigation bias keeps continue. Thus, no land mark matching or any manual operations are made before and in the wind derivation process. But, in 24 hours after orbital and attitude control, the image navigation accuracy is poor. Researches are still going on aimed at reducing bias after orbital and attitude control.

The GAC data of NOAA AVHRR is used to inter-calibrate FY-2 data. CH4 and CH5 from NOAA-17 were used for calibrating FY-2 IR1 and IR2. The CHs 12 and 13 (WV) of HIRS/3 of NOAA-17 are used to calibrate FY-2C WV channel (IR 3). CH 3 of NOAA-17 is used to calibrate the medium wave IR of FY-2C (IR 4). Radiation correction coefficients between FY-2 and NOAA are calculated at the laboratory calibration stage of FY-2. The geometry matching is performed to choose comparison samples for inter-calibration. Comparison pares are taken from similar observation time, location and view angle. Statistics are made with digit count (DC) as input

and radiance temperature as output. It is tried to make radiance temperature histograms compatible between FY-2 and NOAA for the comparison examples.

## 2. FY-2C AMV Retrieval Schemes

The major components of the NSMC processing include tracer selection, tracer tracking, height assignment and horizontal consistence examination. In height assignment component, distinction between high and low clouds is made before height adjustment by correlation between the IR and WV matching templates; Quality control is an integral part of the processing.

### 2.1 Tracer Selection

The maximum correlation method that is used for the tracking of features follows patterns rather than individual cells of cloud or water vapor. No effort is made to choose individual cells. Tracers are simply selected at each 1-degree latitude and longitude grid locations both in the infrared (IR) and water vapor (WV) in the central image of three consecutive images. The operational processing area extends from 50°N to 50°S and  $\pm 50^\circ$  in East- West direction from the sub-satellite point, which leads to 101×101 candidate tracers for one image triplet per channel. 99×99 tracers are effective.

### 2.2 Tracer Tracking

Nominal projection images are used in AMVs derivation.

The tracer tracking of the NSMC scheme adopts a stepwise search with a constraint on consistency in time. With about one third of all possible computations, the stepwise search procedure produces almost same results as full calculation of the complete matching surface. Simultaneously the applied constraint on consistency in time ensures that the smoothest flow is followed.

The search area consists of 96×96 pixels around the center of the matching template. This size ensures that wind speeds of 80 m/s at the sub satellite point can be tracked.

Since the maximum correlation method is quite computer time intensive, correlation calculations are not performed at all locations in the search area. Instead an intelligent calculation procedure is used adopting a stepwise search consisting of 3 steps. In the first step correlation calculations are performed for every 4th line and element location. In the successive steps a refined correlation surface is calculated around the six largest local maxima of the previous step, first at every second and finally at every possible location. At the end of the correlation calculations the pixel position of the maxima and the largest secondary peak are kept. Typically this strategy search reduces the computer time to less than one third of the time needed for the full correlation. The displacements are not significantly different as more than 99.8% have the same tracking results. The stepwise search procedure makes the NSMC AMV derivation scheme independent from NWP since it does not use NWP forecast winds as first guess for the displacement, and thus provides truly independent data from the NWP wind field.

In dark areas on water vapour image, cross correlation is often failed at tracing. For those areas in water vapour images, Euclidean distance is used at tracing (Dew G Holmlund H Logica 2000).

The absolute maximum and secondary peaks (if present) at two successive image pairs are used to identify potential displacement vectors. The vectors derived from the first image pair are compared to the vectors derived from the second image pair. The most consistent vector pair is selected as the final displacement of the tracer. The displacements are calculated with spherical triangle formulae:

Let  $\varphi_0, \varphi_1, \lambda_0, \lambda_1$  represent the latitudes and longitudes for initial and terminal times respectively.  $\Delta\lambda$  and  $\Delta t$  are longitudinal and time differences between initial and terminal positions (time) of the tracer. If  $r_p$  is earth radius at the pole and  $\varepsilon$  is eccentricity of earth the spheroid radius of the Earth ( $r$ ) is defined by:

$$r = r_p + \sqrt{(1 + tg^2 \varphi) / (1 + tg^2 \varphi - \varepsilon^2)} \quad (1)$$

The earth center angle for initial and terminal positions of the tracer ( $\gamma$ ) is defined by

$$\gamma = \cos^{-1}(\sin \varphi_0 \sin \varphi_1 + \cos \varphi_0 \cos \varphi_1 \cos \Delta\lambda) \quad (2)$$

Whereby the wind speed  $FFF$  in m/s and the wind direction  $DDD$  in degrees can be expressed as:

$$FFF = \gamma \cdot r / \Delta t \quad (3)$$

$$DDD = \cos^{-1}[(\sin \varphi_1 - \cos \gamma \sin \varphi_0) / (\sin \gamma \cos \varphi_0)] \quad (4)$$

In case of  $\lambda_1 < \lambda_0$ ,  $DDD = 360 - DD$

A final check at this stage of the processing derives the vector difference of the two selected vectors. If the norm of the vector difference is greater than the mean of the norm of the two vectors, this tracking has failed and the vector is rejected.

### 2.3 Height Assignment for IR winds

In order to separate high level clouds from the low-level clouds, the correlation between the IR and WV matching template is calculated before the height assignment. For tracers with high clouds, the correlation between the IR and WV measurements will be high, whereas for tracers with low clouds it will be low. This information is of major importance to the height assignment. For low correlation cases the height adjustment procedure is not performed.

Tracers with a WV EBBT > 252 K, WV EBBT measurement range < 5K and IR/WV EBBT slope less than 0.35 are defined as low clouds and are not height adjusted.

The height assignment of opaque clouds is based on the IR cloud brightness temperature. For semi transparent clouds, the height assignment method follows the physical principle introduced by Szejwach (1982) by using both IR and WV channels.

Opaque cloud radiation is calculated with NWP data by using atmospheric radiation correction look up table. MODTRAN is used to create atmospheric radiation correction look up tables. The atmosphere is divided into 53 layers. In each layer, atmospheric conditions are constructed by the combination of 11 temperature and 11 humidity measurements. In each layer with each atmospheric status, the atmospheric optical depths in the layers are gained by integration with MODTRAN. In the integration, the atmospheric optical depths are consists of three major parts: water vapour line absorption/emit, water vapour continuous absorption/emit and absorption/emit by other atmospheric compositions. The spectrum resolution in the integration is wave number with unit cm<sup>-1</sup>. The integration spectrum scope is from 700 to 1200 for IR channel and from 1300 to 1600 for WV channel.

In operation, atmospheric radiation correction is gained by using look up tables. A set of atmospheric profiles in 17 layers is received from T213 Numerical Weather Prediction Model (NWP) of National Meteorological Center (NMC) China Meteorological Administration (CMA). Those data are inserted to 53 layers. By using look up table, atmospheric radiation corrections from each layer to the top of the atmosphere for IR and WV channels and then the IR and WV channel Brightness temperature for opaque clouds at different layers are gained. Opaque cloud IR and WV channel Brightness temperature relationship is combined with IR-WV statistical relationship in the image segment to get semi transparent cloud correction. In case no crossing point is gained, the lowest temperature layer ( tropopause ) is assigned.

### 2.4 Height Assignment for WV winds

For WV winds, height is assigned at 85% brightness temperature level.

### 2.5 Horizontal Consistency Examination

During the tracking procedure the NSMC scheme performs a time consistency check that ensures that the smoothest tracking over time is chosen. After the height assignment the NSMC scheme also performs a comparison with surrounding vectors to ensure that horizontal consistency is maintained as much as possible. In the horizontal consistency examination, it is assumed that AMVs are horizontally consistent and should represent a motion at a single level of the atmosphere. The examination is performed at three levels: high (above 399 hPa), middle (between 400 and 699 hPa) and low (below 700 hPa). The examination considers two grids ( $\pm 2$  degrees of longitudes and latitudes) around the AMVs. For each AMV, a Neighboring Mean Vector (NMV) is calculated by the vectors in the examination area and in the layer except the examined AMV itself. The inner grids are given a weight 1 and the outer 0.25. If the sums of all weights exceed 3.0, a Horizontal Coincidence Index (HOI) is calculated with formula developed by Wu (1995):

$$HOI=1 - NMV \times \cos(\Delta DDD)/MAX(AMV,NMV) \quad (5)$$

where  $\Delta DDD$  is the direction difference between AMV and NMV.

The value of HOI ranges from 1 to 0, where a value equals 1 if a vector is totally consistent with the neighboring wind vectors. AMVs with HOI equal to 0 are totally different from the neighboring wind vectors. AMVs with HOI > 0.5 pass the horizontal consistency examination and are given a quality index 0 and those with a HOI < 0.5 fail the examination and are given a quality index 1.

Additionally to the HOI criteria of 0.5, the following AMVs are rejected

- AMVs with speed greater than 18 m/s and  $\Delta DDD > 45$  degree
- AMVs with speed less than 18 m/s and  $\Delta DDD > 60$  degree
- AMVs with sums smaller than 3.0, as it is argued that there are not enough vectors around the AMV in the layer.

Tracers with a very small dynamic range of measurements contain often very thin clouds, either thin cirrus or thin low clouds. In the tropics, the cirrus outflow from convective cloud clusters becomes thinner and thinner before evaporating. The extremely thin cirrus is still traceable, but it is difficult to be separated from low clouds. Therefore tracers with an IR EBBT measurement range less than 5 K or with a WV range less than 2 K are not given a height and are not part of the initial computation of the HOI. These AMVs as well as AMVs rejected at any one-layer horizontal consistency examination are given a quality equal to -1. In a second iteration of the horizontal consistency examination, these vectors may be re-inserted (in the case of HOI > 0.5) and are assigned a height consistent with the mean height of the neighboring AMVs.

## 2.6 Quality Index

Follow the definition of EUMETSAT AMV QI, quality index (QI) of FY-2C AMVs is written as:

$$QI = 1 - \frac{1}{\sum W_i} \sum W_i \cdot \Phi_i \quad (6)$$

$\Phi_i$ ,  $W_i$ , and  $i$  in formula (6) are defined in table 1.

Element( $i$ )	Function( $\Phi_i$ )	Weighting ( $W_i$ )
1 AMV direction time difference	$\frac{ D_2(X, Y) - D_1(X, Y) }{180 + 1}$	1
2 AMV Speed time difference	$\frac{ S_2(X, Y) - S_1(X, Y) }{[S_2(X, Y) + S_1(X, Y)] + 1}$	2
3 AMV Vector time difference	$\frac{ \vec{V}_2(X, Y) - \vec{V}_1(X, Y) }{[S_2(X, Y) + S_1(X, Y)] + 1}$	2
4 AMV Vector space difference	$\frac{1}{n} \sum \frac{ \vec{V}(X, Y) - \vec{V}(X \pm i, Y \pm j) }{[S(X, Y) + S(X \pm i, Y \pm j)] + 1}$	4
5 Deviation from NWP	$\frac{ \vec{V}(X, Y) - \vec{F}(X, Y) }{[S(X, Y) + FS(X, Y)] + 1}$	2

AMV direction D (Unit Degree) AMV Speed S (Unit m/s) AMV Vector  $\vec{V}$  (Unit m/s) NWP Vector  $\vec{F}$  (Unit m/s), NWP Speed FS (Unit m/s)

AMV is one of the FY-2C products. From 1 June 2005 on, FY-2C produces products. From 25 Nov 2005 on, BUFR code of FY-2C AMV is transmitted through GTS. Except for eclipse period, FY-2C AMV is derived 4 times a day. During eclipse period, mid night images are not taken, FY-2C AMV is derived 3 times a day. For each channel and a set of image,  $99 \times 99 = 9801$  winds are derived. Fig. 1 is an example of FY-2C wind distribution for 0529Z, 27 Feb, 2006.

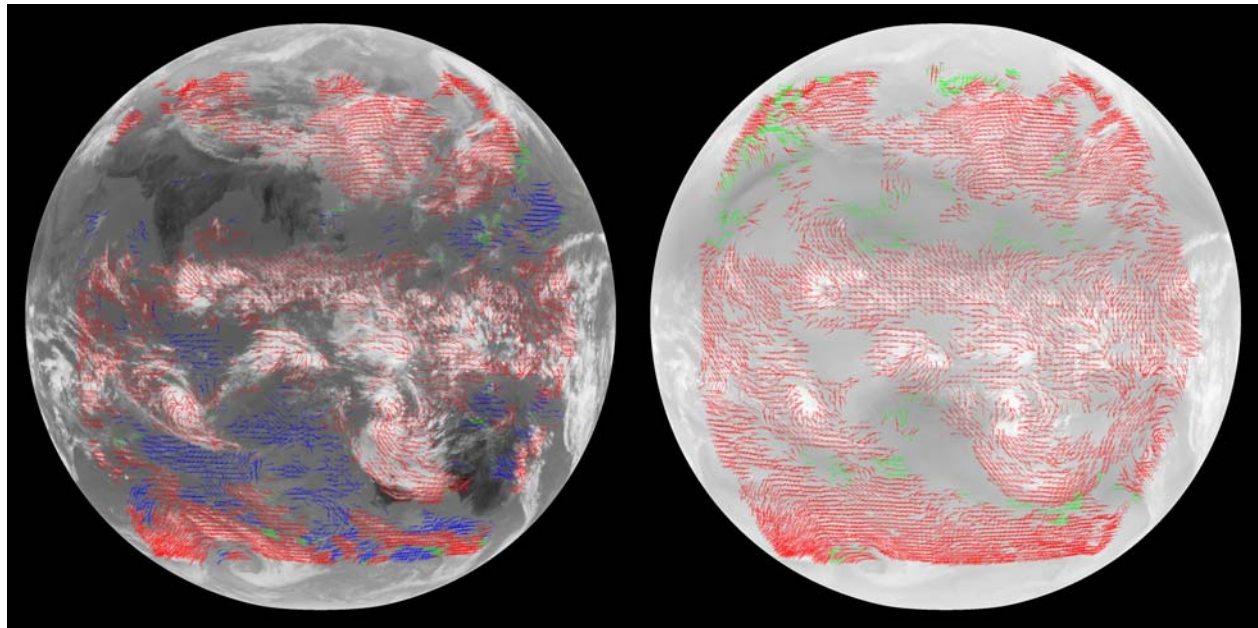


Fig. 1 An example of FY-2C wind distribution for 0529Z, 27 Feb, 2006, Left IR, Right WV

Table 2 shows monthly statistics on FY-2C AMV derivation and wind number derived. To express the density and distribution of FY-2C wind product, the number of winds is divided by the number of derived shown in percentage. From table 2, it is noticed that in November 2005, both the wind data availability and the wind number for each image pair reduced. This is due to the image navigation problem. The image navigation problem was solved on 15 Dec, and the data availability recovered. On 10 Feb. 2006, the coefficients in the AMV derivation algorithm are adjusted, and the wind data distribution improved. On the whole, NSMC AMVs cover 70% area with  $1^\circ \text{Lat.} \times 1^\circ \text{Lon.}$  density.

Table 2 FY-2C operation status

Month	Wind derivation availability (Unit: image pares)						Wind number for each image pare			
	IR			WV			IR		WV	
	Gain	Planed	%	Gain	Planed	%	Number	%	Number	%
200506	119	120	99.17	119	120	99.17	879411	74.77	864559	73.50
200507	121	124	97.58	121	124	97.58	893094	73.49	1215324	70.75
200508	117	117	100.00	104	117	88.89	852017	74.30	1146717	63.22
200509	86	90	95.56	86	90	95.56	628535	71.26	613873	69.59
200510	105	110	95.45	105	110	95.45	784524	72.77	742123	68.84
200511	112	120	93.33	95	120	79.17	811517	69.00	649519	55.23
200512	122	124	98.39	94	124	75.80	885444	72.86	635488	52.29
200601	123	124	99.19	113	124	91.13	897435	73.84	732997	60.31
200602	106	110	96.36	106	110	96.36	809618	75.10	716705	66.48
200603	90	93	96.77	90	93	96.77	726873	79.75	911493	74.83

### 3.2 Comparison with radio sonde reports

Monthly comparisons of FY-2C AMVs with radio sonde data for all AMVs broadcasted are made. Data pairs are chosen in  $1^\circ \text{Lat.} \times 1^\circ \text{Lon.}$  horizontally and 30hPa vertically. Comparison results are shown in Fig. 2 and

tables 2-4. Fig. 2 is difference distribution histogram for March 2006, table 3-5 show mean vector difference and absolute difference.

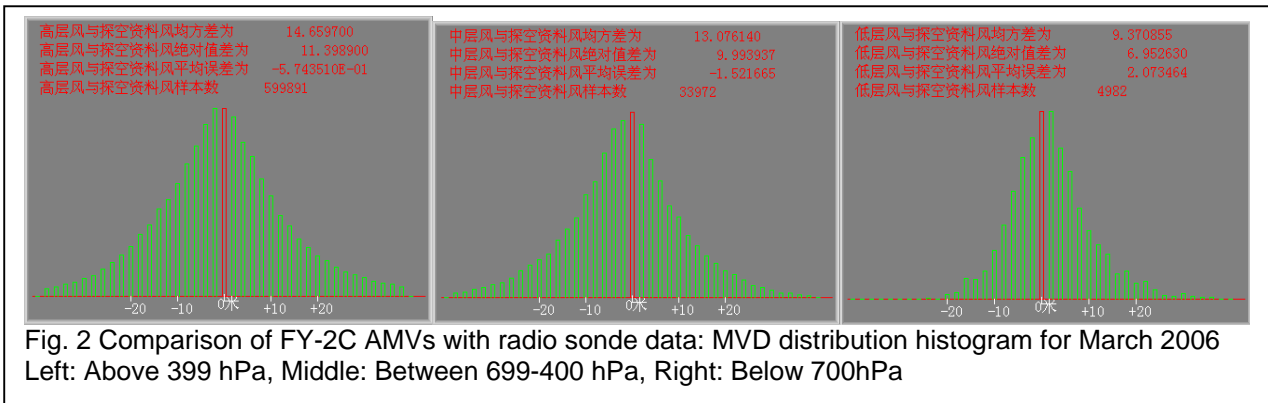


Table 3 Comparison of FY-2C high level (above 399hPa) AMVs with Radio sonde data

	IR High Level Wind				WV High Level Wind			
	Pair Number	Mean Speed	Mean Vector Difference	Absolute Difference	Pair Number	Mean Speed	Mean Vector Difference	Absolute Difference
200506	71528	26.82	12.47	9.36	98143	28.62	13.02	9.91
200507	122103	26.12	12.46	9.43	132572	28.78	12.99	9.93
200508	141184	25.84	12.16	9.14	146659	28.08	12.67	9.59
200509	92251	27.41	12.47	9.48	133451	29.85	13.09	9.97
200510	147134	26.48	12.29	9.09	174594	28.51	12.90	9.74
200511	60613	26.38	13.72	10.25	146909	29.73	14.23	10.80
200512	122025	28.01	13.08	9.73	149824	30.71	14.12	10.74
200601	155921	29.12	14.03	10.62	275090	31.90	14.22	10.91
200602	301676	28.52	15.08	11.59	306523	32.75	14.59	11.16
200603	208088	26.35	14.70	11.58	314740	29.81	14.41	11.06

Table 4 Comparison of FY-2C Middle level (699-400hPa) AMVs with Radio sonde data

	IR Middle Level Wind				WV Middle Level Wind			
	Pair Number	Mean Speed	Mean Vector Difference	Absolute Difference	Pair Number	Mean Speed	Mean Vector Difference	Absolute Difference
200506	4890	25.07	12.91	9.83	8537	27.34	14.16	11.05
200507	11496	26.25	12.17	9.06	12147	29.34	13.73	10.59
200508	15361	26.38	12.13	9.01	18358	27.95	13.30	10.18
200509	11144	26.47	12.41	9.36	15653	29.19	13.75	10.54
200510	15491	22.56	11.84	8.84	16108	27.70	12.60	9.58
200511	7456	20.30	12.91	9.62	11616	25.39	13.74	10.57
200512	15880	24.28	14.78	11.20	10481	26.88	14.98	11.49
200601	15774	22.25	13.68	10.26	18906	25.65	14.02	10.69
200602	11262	20.11	10.09	7.31	19099	23.38	13.11	9.97
200603	5406	20.45	10.12	7.36	26665	23.50	13.49	10.38

Table 5 Comparison of FY-2C low level (below 699hPa) AMVs with Radio sonde data

	IR Low Level Wind			
	Pair Number	Mean Speed	Mean Vector Difference	Absolute Difference
200506	14769	18.52	9.53	7.03
200507	22502	20.18	9.91	7.28
200508	33971	19.38	9.14	6.79
200509	20699	19.01	9.67	7.02
200510	25710	18.28	9.17	6.71
200511	10932	17.14	9.12	6.45
200512	20049	19.59	10.13	7.24
200601	18142	17.25	9.19	6.54
200602	8478	17.12	8.06	5.92
200603	4179	17.95	8.74	6.51

### 3.3 Geometric issues

Image navigation quality influences AMV derivation greatly. FY-2C needs to take orbital and attitude control in about 45 days. Since image navigation depends on historical earth disk center positions, in one or two days after orbital and attitude control, image navigation quality degrades. This is the main reason of unsuccessful processing or quality degradation of AMVs. Measures to improve image navigation quality after orbital and attitude control are under testing.

In FY-2C data processing scheme, after image navigation and calibration, Images are projected to nominal projection. This data processing scheme does make the processing of many products, such as cloud classification etc., more convenient. But AMV derivation is so sensitive to the geometry of image, the adoption of nominal images in AMV derivation is not success. In the future, FY-2C AMVs will be derived based on original images, rather than nominal ones.

### 3.4 Height assignment issues

Height assignment is still one of the major uncertainty factors. Thin cirrus is good tracer. But for thin cirrus targets, IR and WV measurements have small variability. The crossing point position of the IR/WV regression straight line and the opaque cloud curve for thin cirrus targets is uncertain. This is one of the error sources. On the other hand, in case no cross point is gain, the lowest temperature layer ( tropopause ) is assigned as height of AMVs. For T213 NWP Model of NMC/CMA, physical process in southern hemisphere is not well considered, AMV heights may be assigned to a very high level. This is one other error source of NSMC AMVs at present.

### 3.5 NWP and weather forecast application issues

FY-2C AMVs are tested at the simulation of GRAPES model. It is shown that after height adjustment, the usability of FY2-C AMVs is greatly improved. The simulation test status will be presented in one other paper at this conference.

NSMC AMVs are overlapped on the FY-2C imageries and broadcasted to weather forecast offices. Those imageries are welcome by the forecasters.

## 4. Conclusion and future work

The performance of AMVs reflects the overall effect of satellite system and NWP system. To have high quality AMVs to be produced, both the satellite system and the NWP system should be well performed. Image navigation, calibration and NWP are all sensible issues which affect AMV performance. Height assignment scheme still should improve.

In the future, NSMC will work at the following fields to improve AMV quality:

- To improve image navigation, especially after orbital and attitude control;
- To improve calibration;

- To use height adjustment method in height assignment;
- To test geometry height assignment method;
- To have interaction with NWP.

## 5. References

- Dew G Holmlund K 2000 Investigations of cross-correlation and Euclidean distance target matching techniques in the MPEF environment Proceedings of the fifth International Winds Workshop Lorne 28 February - 3 March EUMETSAT EUM P 28 235 – 243
- Holmlund K Velden C S Rohn M 2001 Enhanced automated quality control applied to high-density satellite-derived winds Mon. Wea. Rev. 129 517 – 519
- Schmetz J Arriaga A Holmlund K 1998 Sensitivity of the height allocation of thin cloud tracers in satellite calibration Proceedings of the 4th International Winds Workshop Saanenmöser Switzerland 20 – 23 October 1998 EUMETSAT Publication EUM P24 225-231
- Szejwach G 1982 Determination of semitransparent cirrus cloud temperature from infrared radiances application to meteosat Journal of Applied Meteorology 21(3) 384-393
- Alan V Di Vittorio William J Emery Senior Member. An Automated Dynamic Threshold Cloud-Masking Algorithm for Daytime AVHRR Images Over Land. IEEE Transactions on Geoscience and Remote Sensing 2002 VOL.40 NO.8 August.
- Xu Jianmin Zhang Qisong 1996 Calculation of cloud motion wind with GMS-5 images in China Proceedings of the Third International Winds Workshop Ascona 10-12 June 1996 EUMETSAT Publication EUM P18 45-52
- Xu Jianmin Zhang Qisong Fang Xiang Liu Jian 1998 Cloud motion winds from FY-2 and GMS-5 meteorological satellites Proceedings of the 4th International Winds Workshop Saanenmöser Switzerland 20 – 23 October 1998 EUMETSAT Publication EUM P24 41-48
- Xu J Holmlund K Zhang Q Schmetz J 2002 Comparison of two schemes for derivation of atmospheric motion vectors Journal of Geophysical Research 107(D14)
- Xu J Lu F Zhang Q S 2002 Automatic navigation of FY-2 geosynchronous meteorological satellite images Proceedings of the 6th International Winds Madison wisconsin USA 7-10 May 2002
- Xu Jianmin Zhang Qisong etc. 2004, Recent works aimed at operational FY2C AMVS Proceedings of the 7th International Winds Helsinki Finland 14-17 June 2004